16th Australasian Fluid Mechanics Conference
Crown Plaza, Gold Coast, Australia
2-7 December 2007

Particle Image Thermometry for Natural Convection Flows

T.P. Bednarz, C. Lei and J.C. Patterson

School of Engineering, James Cook University
Townsville, QLD 4811, AUSTRALIA

Abstract

Particle Image Thermometry (PIT) is a technique by which temperature fields can be obtained non-invasively using thermo-chromic liquid crystals (TLCs) through image processing of experimental true-colour photographs. This is done using a calibration curve (hue versus temperature). With the calibration data, every pixel of the colour photograph is transformed to a temperature value, and thus accurate experimental temperature maps are obtained. Using this technique, examples of steady and unsteady natural convection are presented, which include steady magnetic convection of paramagnetic fluids in a cubic enclosure heated and cooled from opposite walls, and unsteady convective flows in a reservoir model cooled from above (night-time cooling). The instantaneous measurement of temperature fields is very useful for understanding flow characteristics in situations where conventional flow visualisation is not sufficient. This method also provides additional quantitative information for comparisons with numerical modelling.

Introduction

TLCs (Thermo-chromic Liquid Crystals) are widely used in science and engineering to map temperature distributions in fluids or on rigid surfaces. They usually exist in the smectic, the nematic or the cholersteric (also chiral nematic) phases [1, 2]. When a white light source shines on the chiral nematic TLC, light of only one particular wavelength corresponding to the temperature is reflected. Thus, this property is used to measure accurately the temperature by observing the reflected wavelengths (or colours). The visible colour of TLCs turns from colourless (black against a black background) to red at a given temperature. As the temperature is increased, the TLCs' colour passes through other colours of the visible spectrum in sequence (orange, yellow, green, blue, violet) before turning colourless again at a higher temperature [3, 4]. These colour changes are repeatable and reversible, as long as the TLCs are not chemically degraded or physically damaged. TLCs therefore can be calibrated accurately against known temperatures and used as temperature indicators. The response time of TLCs is 3 ms which is short enough for typical thermal problems in fluids. TLCs are normally clear or slightly milky in appearance and change their colour over a narrow range of temperatures. Their colour-temperature play range depends on the TLC composition prepared during the manufacturing process, and can be selected for bands of about 0.5ºC to 20ºC with working temperatures ranging from -30ºC to above 100ºC [5]. The suspension of thermochromic liquid crystals can be used not only for temperature visualization but also for velocity estimations through the method of particle tracking [2, 6].

Temperature Field Measurements

Accurate temperature measurements using thermo-chromic liquid crystals are based on a colour analysis of the RGB (Red-Green-Blue) colour components of digital images taken by a hi-resolution digital camera. The key point of this method is to find a unique function of the set of three colour components (R, G, B) for a given temperature and construct a temperature calibration curve. It is possible to do so using R, G and B colour components. However a more favourable method from the physical point of view is available for that purpose. With this method, the RGB colour space is transformed into another trichromic decomposition called HSI (Hue, Saturation and Intensity). In such colour space, the hue (H) represents the dominant colour related directly to a specific spectral wavelength of the light, and it is the most appropriate measure of the colour corresponding to the spectral analysis of the reflected light. The intensity (I) represents the physical brightness of the light and the saturation (S) represents the purity of the colour. The HSI colour model uses a hue value of 0 degrees to 360 degrees, with the red colour at 0, yellow at 60, green at 120, cyan at 180, blue at 240 and magenta at 300. Saturation is in the range of 0 to 1, with 0 being no colour (gray) and 1 being full colour. The intensity also has a range of 0 to 1, where 0 is black and 1 is white. For example, by maintaining S = 1 and adjusting I, shades of the colour can be created.

One possible transformation from RGB to HSI space is given by the following equations [7]:

$$H = \begin{cases} \theta & \text{if } b \le g \\ 360 - \theta & \text{if } b > g \end{cases} \tag{1a}$$

where:

$$\theta = \cos^{-1}\left\{ \frac{0.5 \cdot [2r - g - b]}{\left[(r-g)^2 + (r-b)(g-b)\right]^{0.5}} \right\} \tag{1b}$$

The intensity I can be computed using the following formulae:

$$I = \frac{1}{3}(r + g + b) \tag{2}$$

Finally, the saturation S is given by

$$S = 1 - \frac{min(r, g, b)}{I} \tag{3}$$

where $r = R/(R+G+B)$, $g = G/(R+G+B)$ and $b = B/(R+G+B)$ are normalized RGB values.

The most critical part of the TLCs based thermography is to obtain the hue-versus-temperature relationship. The observed colours depend on the observation angle, the scattering properties of the tracers, colour and refractive index of the immersing liquid. Therefore it is very important to carry out the experiments carefully and always in the same light conditions, with the same fluid and if possible with exactly the same experimental setup as those for the calibration.

Two different calibration techniques are presented below: the first using a conduction experiment and the second using series of photographs done at several temperatures throughout the TLCs temperature indication range. Following these calibrations, selected results from natural convection experiments are presented.

Calibration: Conduction Method

Figure 1 shows the experimental apparatus used for conduction calibration. Later, the same cubical enclosure was used to carry out steady magnetic convection experiments. The presented apparatus was assembled from five separate elements. These included two copper plates (one for the cooling side, the other for the heating side) with three holes in each plate for inserting the T-type thermocouples, the cubic cavity made of Plexiglas with a hole for filling the working fluid, and the cooling and heating chambers made of Plexiglas. The cooling copper plate was cooled by the water flowing through the chamber pumped from a circulator, whereas the heating copper plate was heated by a nichrome wire covered with a rubber and winded in the heating chamber. The internal dimension of the cavity was 0.032 m for each side.

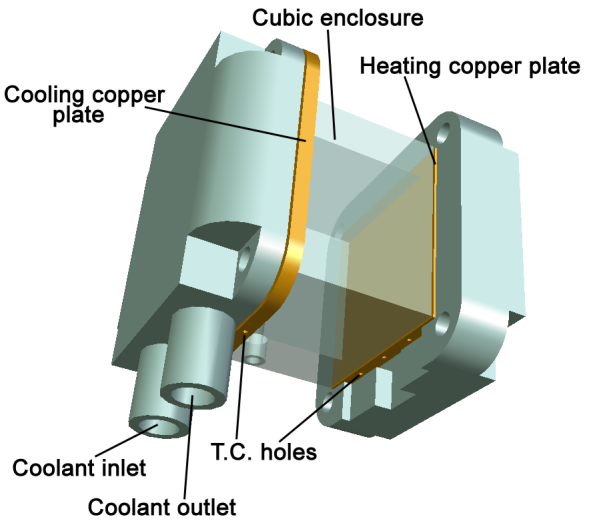

Figure 1. Experimental apparatus.

The working fluid in the cubic enclosure was filled using a syringe and a thin needle. The filling hole was later sealed by silicone resin to avoid leakage of the fluid through it. The syringe was also very useful for removing unwanted air bubbles which sometimes were present in the enclosure. An 80% mass aqueous glycerol solution was employed as a working fluid. This was additionally mixed with crystals of gadolinium nitrate hexahydrate to make it paramagnetic. The thermophysical properties of the fluid can be found in [8, 9]. A small amount of liquid crystal slurry (KWN-20/25, Japan Capsular Products) was added to the fluid for flow visualization.

Figure 2a illustrates an example of the calibration curve obtained for the TLCs used in studying magnetic convection in a cubical cavity. The curve was obtained from a conduction experiment (with the fluid cooled from below and heated from above) after a steady linear temperature stratification was established in the cube. The hue evaluation was performed for each pixel under constraints of the minimum and maximum pixel intensities and the minimum saturation. Only "good" pixels for which the angle θ was defined [10] were used to build the calibration curve and later that curve was used for qualitative estimation of the temperatures from the convection experiments. An example of the application of the calibration curve is shown in Figure 2b. The photograph from the convection experiment was taken from the same distance as the photo from the conduction experiment; the same white-balance was used, and the same filtering procedures were applied for every pixel of the photograph. It is seen in Figure 2 that, using the calibration curve, it was possible to convert a colour photo into a qualitative map of the temperature field.

Calibration: Point by Point Method

Figure 3 shows the UML (Unified Modeling Language) diagram of the experimental setup used to investigate unsteady natural convection in reservoirs. The main part of the experimental setup is the experimental model, a cross section of which is shown in the figure. The experimental model consisted of four separate parts: an enclosure, a cooling chamber (both made of transparent Perspex of a thickness 0.006 m), a slope (made of transparent Perspex of a thickness 0.015 m) and a copper plate. The cavity was 0.3-m long in total, 0.06-m wide and 0.015-m high. A slope of an inclination A = 0.1 (horizontal length 0.15 m, width 0.06 m and height 0.015 m) was placed inside the enclosure and fixed to the walls. The upper part of the apparatus was the cooling chamber with two separate coolant outlets and two separate coolant inlets, each located at the center of a specific side wall of the cooling chamber. The copper plate of a thickness 0.002 m, a length 0.31 m and a width 0.07 m was attached at the bottom of the cooling chamber. On the UML diagram (Figure 3), the arrows/lines represent the connections of the equipment (represented by simple blocks) used in the experiment. As seen in the diagram, the cooling chamber was connected to a thermo-stating water bath controlled by a personal computer (computer A). The tip of the thermistor was placed inside the cavity allowing continuous temperate measurements at a location close to the deep-end wall. The thermistor was connected to a data acquisition system controlled by LabVIEW software on a separate computer (computer B). Before starting the experiment, the cavity was filled with filtered water, and all air bubbles were excluded.

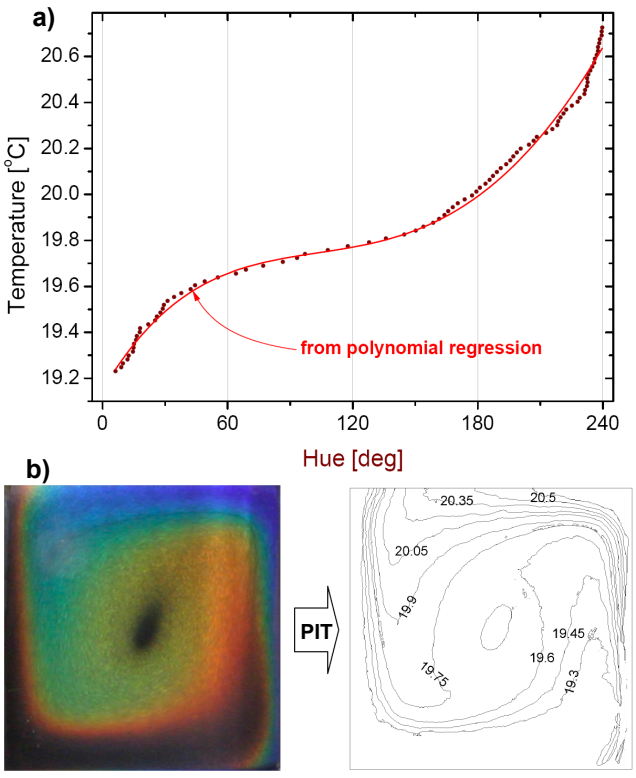

Figure 2. (a) A calibration curve obtained from the conduction experiment; and (b) an example of its application.

Thermo-chromic liquid crystal slurry (KXN-20/30, Japan Capsular Product Inc.) was used to visualize the temperature field inside the cavity. The concentration of the slurry was adjusted for each experiment, but was always less than 1 ppt.

In this experiment, the middle vertical cross-section of the enclosure was illuminated by a white light generated from a

projector lamp, which was located at about 2 m from the mirror placed underneath the enclosure. The horizontal light sheet was reflected by the mirror and then redirected vertically through the entire middle section of the enclosure. Although of relatively low intensity, the light sheet from the projector lamp was sufficient for the flow visualization. Experimental movies were taken by two CCD colour cameras (Basler A102fc) located at about 3 m from the experimental apparatus. In the meantime, series of photographs were also taken by a hi-resolution (6 MPix) SLR digital camera (Canon EOS 10D) with a EF 70-200 f/2.8 IS lens for extracting quantitative information

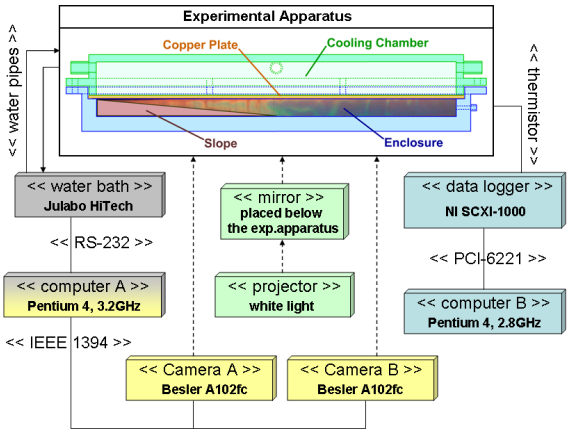

Figure 3. UML diagram of the experimental setup for unsteady natural convection in reservoir.

For the calibration purpose, the water body was cooled to a constant temperature in the range from 24.2ºC to 18.9ºC in 26 steps. At every step, the water was kept at the specified temperature for about 20-25 minutes, and then an experimental photograph was taken. After that, the temperature was set to the next calibration step, and the above procedure was repeated. A sixth-order polynomial regression was used to fit the known temperatures with the corresponding hue values calculated from the RGB colour components (refer to Figure 4a). The polynomial fit was only applied to points within the monotonic region (i.e. for temperatures between 19.7-23.7ºC). The error bars represent the standard deviation in the calculated hue from the region of interests within the measured colour bandwidth of the KXN-20/30. As seen in Figure 4a, there were some variations of the reflected wavelength from the TLC particles at the same temperature. The highest uncertainty occurs at higher temperatures, at which the colour response of the TLCs is entering a transparent regime. The departure of the actual temperature measurements from the ideal correlation is indicated by the coefficient of determination R^2 which is 0.9953, and by the mean absolute error which is estimated to be 0.059ºC in this case.

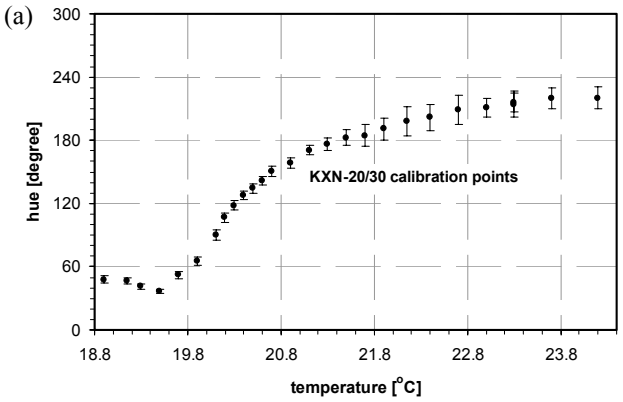

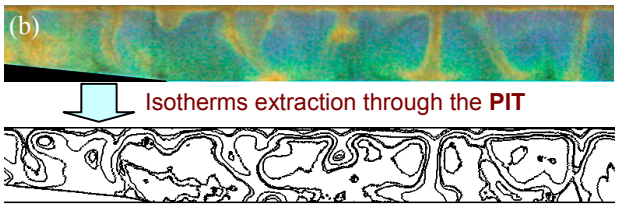

Figure 4. (a) A calibration curve for KXW-20/30; and (b) A sample PIT transformation: from an experimental photograph to the isotherms.

Application – Steady Magnetic Convection in a Cube

In this section, the applications of the TLCs for two different cases of thermally driven steady flows under a strong magnetic field in a cubic enclosure are presented. The experimental apparatus was subject to different configurations of the magnetic field in order to show its effect on the suppression and the inversion of the well known gravitational convection in a cube heated and cooled from two opposite vertical walls. For the PIT analysis, the conduction calibration was used.

For easy characterization of the convection flow, two non-dimensional parameters are defined. They quantify the important fluid and flow properties of the system. These are: the Prandtl number (Pr) which characterizes the ratio of momentum diffusion to thermal diffusion, the Rayleigh number (Ra) which characterizes the strength of the thermal forcing:

$$Pr = \frac{\nu}{k} \tag{4}$$

$$Ra = \frac{g\,\beta\,\Delta T\,L^3}{\nu\,k} \tag{5}$$

where ν is the kinematic viscosity, k is the thermal diffusivity, g is the gravity acceleration, b is the thermal expansion coefficient, ΔT is the initial temperature difference and L is a characteristic length (in this case length of the cube). The strength of the magnetic field is described by b_0, measured at the centre of the magnet's solenoid system.

Suppression of the Convective Flow

Figure 5a shows the isotherms obtained in the case with the magnetic field switched off (0 T) and for $Ra = 9.64\times10^4$, $Pr = 584$. The left-hand side wall is heated and the right-hand side wall is cooled in this case. The temperature profiles resemble the popular benchmark solution [11, 12] that has been used previously to test numerical codes. The gravitational buoyancy force causes relatively warmer fluid to move upwards along the heated wall and then along the top wall towards the cooled vertical wall. The relatively coder fluid moves downward along the cooled wall and then moves toward the heated wall along the bottom wall. As a result, a convective circulation is created. The visualization done with the TLCs allowed identification of the variation of the temperature field. Even without the quantitative PIT profiles, the characteristic of the isotherms could be deducted from the colour photographs. The PIT analysis has given additional meat to the proper understanding of the flow features. The isotherms extracted from the photograph have been used for comparison with the corresponding numerical modelling. The numerical approach for the problem of magnetic convection in terrestrial conditions is presented in [8, 9].

Figure 5b, shows the isotherms strongly affected by the horizontal magnetic buoyancy force. The photograph was made at $Ra = 1.44\times10^5$, $Pr = 584$ and $b_0 = 8$ T. In this experiment, the 10-Tesla magnet is located horizontally on the right with the solenoid centre placed 0.23 m from the centre of the cube (the solenoid is close to the right-hand side cooled wall [13]). The relatively colder fluid is strongly attracted towards the magnet due to its larger magnetic susceptibility, which causes the convective motion to be suppressed. The isotherms become

more inclined (more conduction-like flow is resulted). The corresponding numerical results are consistent with the experimental data.

Inversion of the Convective Flow

Another example of the steady magnetic convection visualized using the liquid crystal slurry (KWN-20/25) is presented in Figure 6. The first photo was shot at 0 T, Pr = 584 and Ra = 8.16×10^4. In this experiment, the left-hand side wall is cooled, and the right-hand side wall is heated. The convective circulation under the pure gravitational effect is created in the same way as that described above.

Figure 6b shows isotherms obtained at 8 T, Pr = 584 and Ra = 7.23×10^4. In this case, the magnet is located vertically and is above the enclosure with the centre of its solenoid placed at a distance of 0.23 m from the centre of the cube. The magnetic buoyancy acts here together with the gravitational buoyancy. However, at the magnetic induction of 8 T, the gravitational force is overcome by the magnetic force, and the convective motion is inversed, as clearly seen in Figure 6b. The cold fluid is strongly attracted towards the magnet position and moves upward along the left-hand side wall and then along the top wall towards the hot wall. On the contrary, the relatively warmer fluid moves downward along the heated wall. The convective circulation is created as in the case of gravitational natural convection, however it circulates in the reverse direction. The experimental results are successfully verified by the numerical modelling presented in Figure 6.

Application – Unsteady Natural Convection in a Reservoir Model

TLCs can also be successfully used in visualizing and measuring unsteady convective flows. The application shown below considers a model of a reservoir cooled from above (refer to Figure 3). The working fluid (water) is initially isothermal, and at t = 0 s, it is subject to cooling from the top surface. The cooling is achieved by circulating water from a thermo-stating water bath of a lower temperature through the cooling chamber. A series of photographs were made in order to observe the transient development of the flow and the evolution of the temperature field. For the PIT analysis in this application, the point-by-point calibration method was used. The convection flow is also characterized by Pr and Ra, defined before in equations 4 and 5. Here L in the definition of Ra is the height of the enclosure for this case.

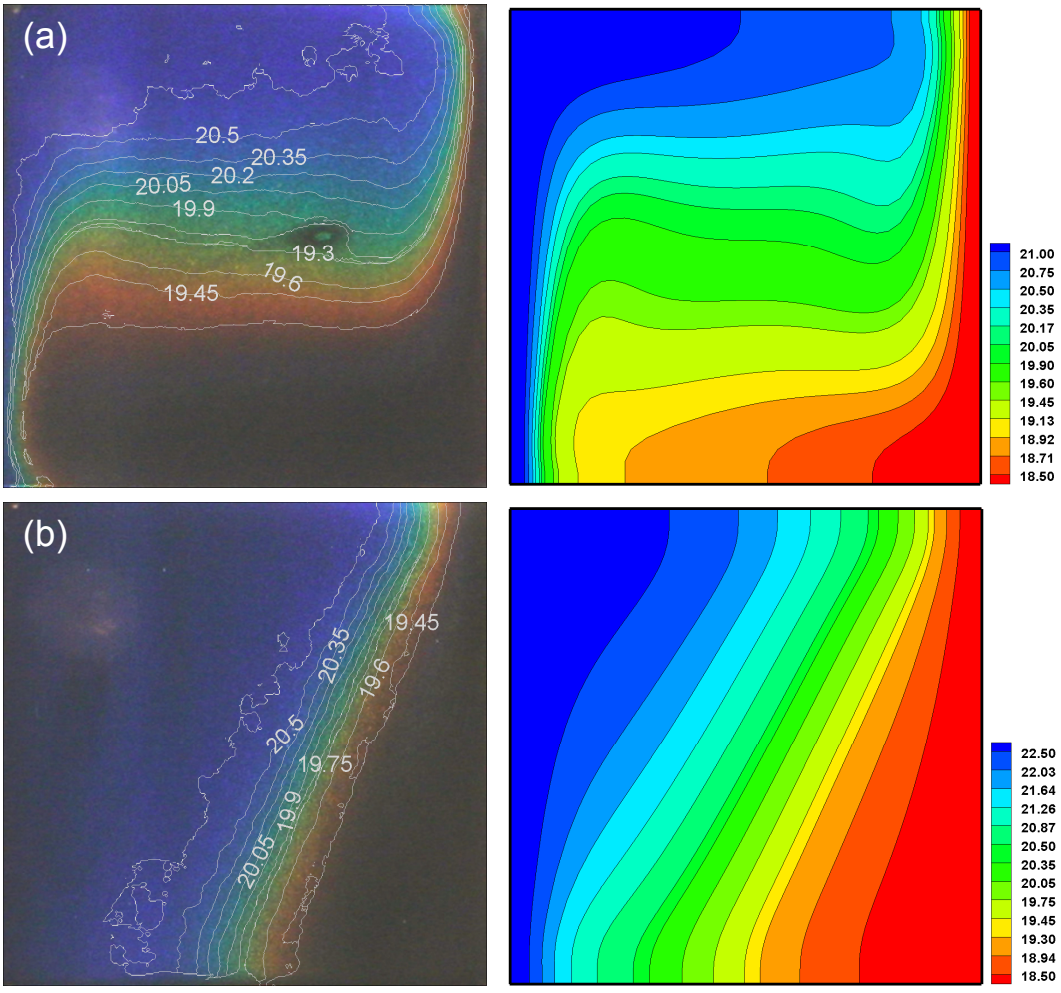

Figure 5. Isotherms. Left: experiment + PIT, right: corresponding numerical simulations. (a) 0 T, (b) 8 T in the centre of the coil. Magnet is placed horizontally on the right-hand side of enclosure.

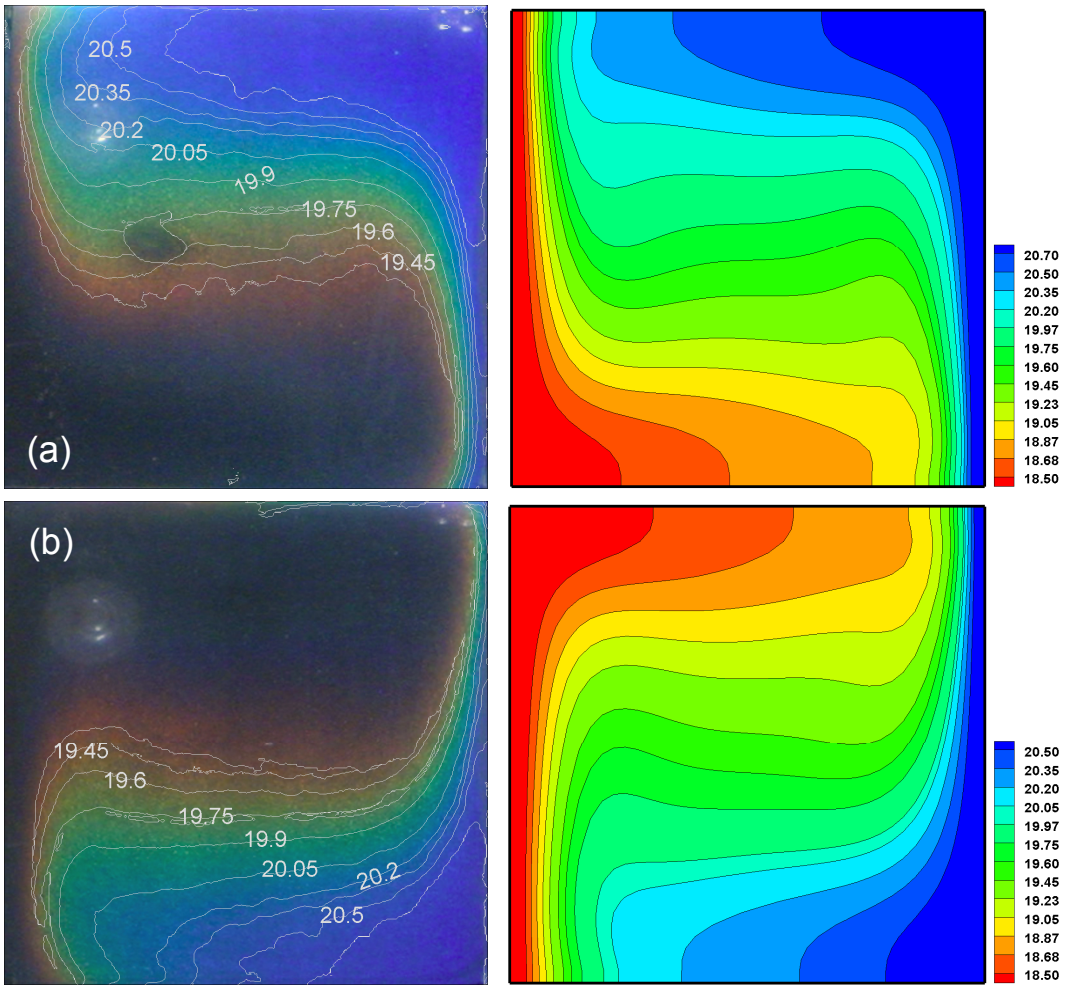

Figure 6. Isotherms. Left: experiment + PIT, right: corresponding numerical simulations. (a) 0 T, (b) 8 T in the centre of the coil. Magnet is placed vertically above the enclosure.

Estimation of the Thermal Boundary Layer

Initially the fluid in the experimental enclosure was stationary and isothermal. As soon as the cooling started, a conductive thermal boundary layer grew underneath the water surface. The thickness of the boundary layer could be measured from the experimental photographs using the PIT technique. Figure 7 plots the growth of the thermal boundary layer thickness with time (triangles), which was measured at a horizontal location of 0.15 m from the tip at $Ra = 5.4\times10^4$, $Pr = 6.91$ (the initial fluid temperature was 21.00 ºC, and the temperature of the top surface was 19.90 ºC). The thickness of the thermal boundary layer was determined based on the hue value of 160 corresponding to a temperature of 20.95 ºC. The dashed line represents a power trend fitting to the points extracted from the analysis. The trend line was calculated to be $\delta_T = 0.6419 \cdot t^{0.499}$ with $R^2 = 0.9956$, therefore good agreement was observed between the experimental data and the theoretical scaling prediction of $\delta_T \sim (\kappa t)^{0.5}$.

Unsteady flow development

Applying the PIT technique to the series of photographs, the transient temperature fields can be obtained. They are good indicators of the flow development. Figure 8 shows the temperature profiles obtained using the PIT technique from the experimental series with $Pr = 7.51$ and $Ra = 4.23\times10^5$ (the initial fluid temperature was 22.90 ºC, and the temperature of the top surface was 12.00 ºC). At the early stage, a horizontal conductive thermal boundary layer is developing under the water surface, as seen at $t = 6$ s. After, a critical Rayleigh number is reached locally, convection instabilities set in. At $t = 18$ s, the early stage of the instabilities in the form of plunging plumes is observed. At $t = 22$ s, the plumes penetrate almost the full depth of the enclosure. These are typical flow phenomena of Rayleigh-Benard convection, which carry colder water toward the bottom, where they are prone to overturning and mixing with the ambient fluid.

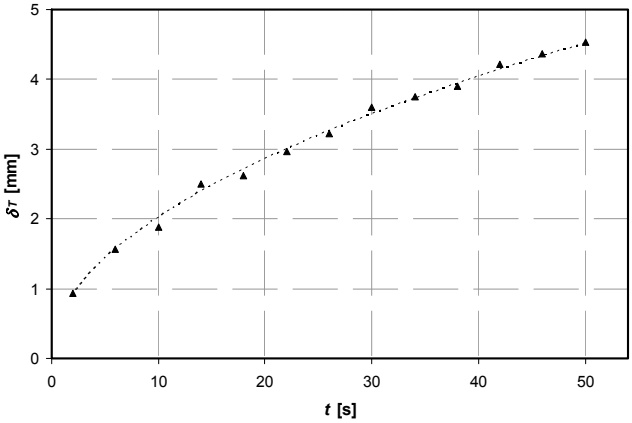

Figure 7. The thickness of the boundary layer δ_T plotted against time and measured at $Pr = 6.91$ and $Ra = 5.4\times10^4$. The dashed line represents the power trend line.

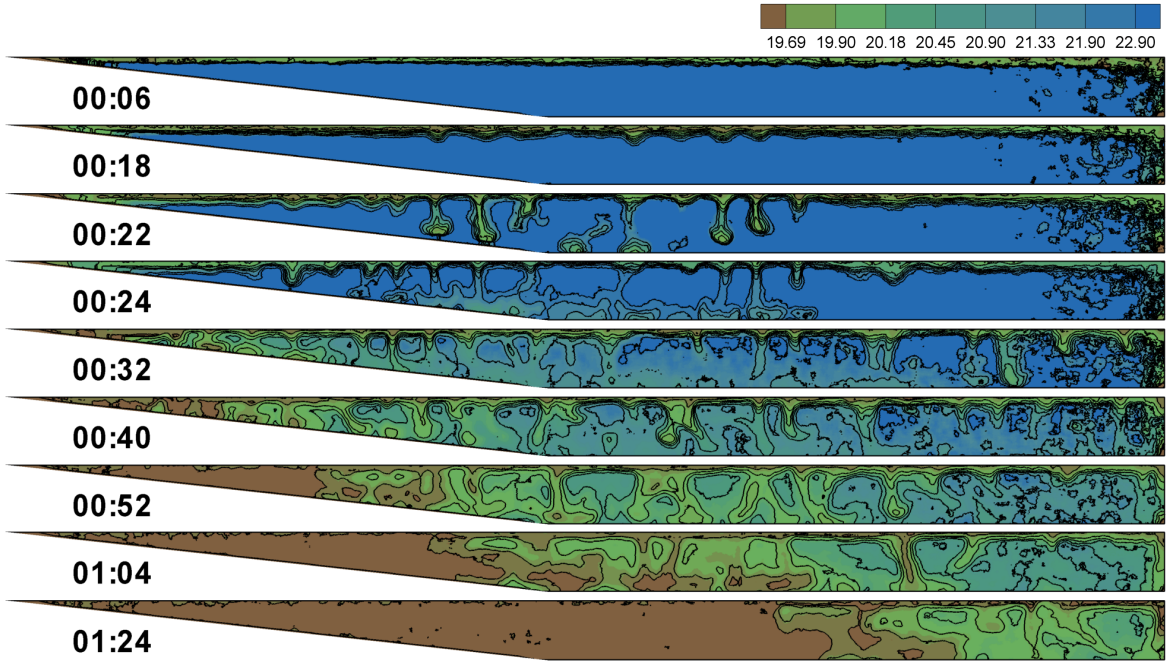

Figure 8. Isotherms obtained using the PIT technique on the series of photographs from the cooling experiment.

Conclusions

The present paper presented a few examples of the TLC application for natural convection flows. Two different calibration methods of the TLCs are also presented: a conduction calibration method and a step-by-step calibration method. Both methods are equivalent and can be successfully used to extract temperatures from series of experimental photographs. In order to minimize the temperature estimation error, ideally the calibration experiments should be carried out with the same model and lighting condition as that in the actual experiments. Therefore, both calibration methods can be successfully applied for the magnetic convection experiments in the cubic enclosure. However, only the point-by-point calibration method is possible for the experiment with the reservoir model or any other model which does not sustain a stable stratification.

Application examples in this paper include the steady magnetic convection in a cube and the unsteady night-time cooling in a reservoir model. As it was demonstrated in this paper, in addition to temperature extraction, the PIT method can also be effectively used for extracting other flow properties such as the thermal boundary layer thickness. The present study has also demonstrated that the PIT analysis can be successfully used to verify numerical modelling.

Acknowledgment

The authors gratefully acknowledge the financial support of the Australian Research Council.

References

[1] Pigon, K. & Ruziewicz, Z., *Chemical Physics – Volume 1*, Wydawnictwo Naukowo Techniczne PWN, 1993, in Polish.

[2] Park, H.G., Dabiri, D. & Gharib, M., Digital particle image velocimetry/thermometry and application to the wake of a heated circular cylinder, *Experiments in Fluids* **30**, 2001, 327-338.

[3] Smith, C.R., Sabatino, D.R. & Praisner, T.J., Temperature sensing with thermochromic liquid crystals, *Experiments in Fluids* **30**, 2001, 190-201.

[4] Fujisawa, N. & Funatani, S., Simultaneous measurement of temperature and velocity in a turbulent thermal convection by the extended range scanning liquid crystal visualization technique, *Experiments in Fluids* [Suppl.], 2000, 158-165.

[5] Stasiek, J.A. & Kowalewski, T.A., TLCs applied for heat transfer research, *Opto-Electronics Review* **10**, 2002, 1-10.

[6] Kowalewski, T.A., Application of liquid crystal tracers for full field temperature and velocity measurements, *Proceedings of the 2001 International Symposium on Env. Hydraulics*, 2001.

[7] Gonzalez, R.C., Woods, R.E. & Eddins, S.L., *Digital image processing using Matlab*, Pearson Education Inc, 2004.

[8] Bednarz, T., Fornalik, E., Tagawa, T., Ozoe, H. & Szmyd, J.S., Convection of paramagnetic fluid in a cube heated and cooled from side walls and placed below a superconducting magnet - comparison between experiment and numerical computations, *Thermal Science & Engineering Journal* **14**, 2006, 107-114.

[9] Bednarz, T., Fornalik, E., Tagawa, T., Ozoe, H. & Szmyd, J.S., Experimental and numerical analyses of magnetic convection of paramagnetic fluid in a cube heated and cooled from opposing vertical walls, *Int. Journal of Thermal Sciences*, 44, 2005, 933-943.

[10] Gonzalez, R.C., Woods, R.E., *Digital image processing*, Addison-Wesley, 1992

[11] De Vahl Davis, G., Natural convection of air in a square cavity: A bench mark numerical solution, *Int. J. Numerical Methods in Fluids* **3**, 1983, 249-264.

[12] De Vahl Davis, G., Natural convection in a square cavity: A comparison exercise, *Int. J. Numerical Methods in Fluids* **3**, 1983, 227-248.

[13] Bednarz, T., Fornalik, E., Tagawa, T., Ozoe, H., Szmyd, J.S., Patterson, J.C. & Lei, C., Influence of a horizontal magnetic field on the natural convection of paramagnetic fluid in a cube heated and cooled from two vertical side walls, *Int. Journal of Thermal Sciences*, 2007, in press.

[14] Lei, C. & Patterson, J.C., Unsteady natural convection in a triangular enclosure induced by surface cooling, *Int.J. Heat and Fluid Flow* **26**, 2005, 307-321.

[15] Lei, C. & Patterson, J.C., Natural convection induced by diurnal heating and cooling in a reservoir with slowly varying topography, *JSME Int. Journal Series B* **49**, 2006.